Zeitschrift: IABSE congress report = Rapport du congrès AIPC = IVBH Kongressbericht

Band: 7 (1964)

Rubrik: IId: Fatigue life of structural members

IId1

Fatigue Life of Bridge Beams Subjected to Controlled Truck Traffic

Résistance à la fatigue de poutres de ponts soumises à des essais de passage de camions

Dauerfestigkeit von Brückenträgern für Testlastenzüge

JOHN W. FISHER
Research Instructor, Lehigh University, Bethlehem, Pa., U.S.A.

IVAN M. VIEST
Structural Engineer, Bethlehem Steel Co., Bethlehem, Pa., U.S.A.

Introduction

Although almost no fatigue failures of highway bridges have been reported, the increasing frequency of heavy trucks on modern highways suggests that the past experience may not be indicative of future trends. A fairly extensive body of laboratory data has been available on the fatigue life of structural members. However, the scarcity of failures in the field left unanswered the question of how to apply the results of the laboratory research to practical design problems, and gave rise to some doubt concerning the need for fatigue considerations in the design of highway bridges.

To explore the subject of the fatigue life of highway bridges, the American Association of State Highway Officials undertook tests of eighteen bridges under repeated overstress. The experiment was a part of the AASHO Road Test, a study of highway pavements and bridges under controlled truck traffic.

The principal objective of the bridge research program was to gather information on the effects of repeated overstress. In the past, many investigations of the fatigue life of beams were made on small laboratory specimens. Such tests covered wide ranges of pertinent variables. Could these laboratory tests be applied to bridges in actual service? Given characteristics of the materials and a reasonable estimate of the number, weight, and arrangement of the vehicle loads, could one make a reasonably good prediction of the usable life of the structure?

The combination of the precise knowledge of the materials, the design of the structures and the control of the loading made possible to study these and other items at the Road Test. The tests afforded the rare opportunity to compare the results of simpler laboratory experiments with the behavior of actual bridge structures. This paper deals only with five bridges with steel beams that showed fatigue distress.

Description of Tests

Bridge Tests

Each superstructure consisted of three steel beams and a reinforced concrete deck. The beams were fabricated from 18-in. deep wide-flange sections rolled of A 7 structural steel. In three bridges the beams were independent of the slab. A treatment of the top surface of the top flanges inhibited formation of natural bond between the slab and the steel beams. In two bridges the steel beams were connected to the slab with channel connections.

Beams of one noncomposite bridge and of the two composite bridges had partial-length cover plates on the bottom flange only, while the beams of the other two noncomposite bridges had partial-length cover plates on both the top and bottom flanges. All plates were welded to the flange with $^5/_{16}$-in. continuous fillet welds along the longitudinal edges. The ends of the plates were square and had no end welds.

The mean yield point of the flanges of the wide-flange beams varied from 32,500 to 37,900 psi and the mean ultimate strength from 59,500 to 64,900 psi from bridge to bridge. The chemical composition of the steel was 0.20—0.24% Carbon, 0.41—0.71% Manganese, 0.007—0.014% Phosphorus and 0.023 to 0.040% Sulfur. The estimated mean residual stresses in the flanges, caused by rolling the wide-flange sections, varied from a compression of 7,400 psi to a tension of 11,300 psi.

Individual mean values of the material properties for a particular beam, bridge, or slab and their standard deviations may be found in an earlier report [1]). The report contains also a description of the test methods and details of the construction procedures.

During a two-year period of test traffic, the bridges were tested with tractor semi-trailer trucks which traveled around the loops at approximately 30 mph. The time interval between individual passages of the vehicles over a bridge varied from one to two minutes. This resulted in over half a million passages of the test vehicles. Details of the test structures and experiments may be found elsewhere [2]).

The maximum stresses in the steel beams occurred just off the ends of the cover plates. The stresses at these critical locations varied during the vehicle trip. A typical variation of stress at the end of a cover plate during the trip of a vehicle over a bridge is illustrated in Fig. 1.

After a vehicle crossed a bridge, the bridge continued to vibrate causing alternate upward and downward deflections of decreasing amplitude. These

---

[1]) "The AASHO Road Test, Report 2, Materials and Construction", *Highway Research Board*, Special Report 61B, 1962.

[2]) "The AASHO Road Test, Report 4, Bridge Research", *Highway Research Board*, Special Report 61D, 1962.

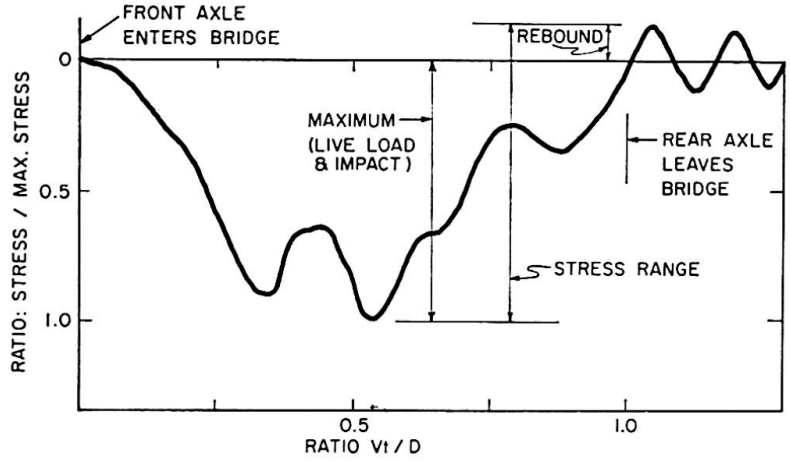

Fig. 1. Variation of stress near end of cover plate on passage of vehicle.

deflections caused stress fluctuations (Fig. 1). The maximum amplitude of the first negative half cycle of the stress fluctuation was designated the rebound stress. The rebound stress was of a sign opposite to that of the stress observed while the vehicle was on the bridge and thus increased the range of the fluctuating stress. The ratio of the sum of the maximum transient stress and the rebound stress to the maximum transient stress was in excess of 1.1 for non-composite bridges and less than 1.1 for composite bridges.

Laboratory Tests

The fatigue characteristics of steel beams with partial-length cover plates with no welds across the end were evaluated by studies of the results of flexural fatigue tests of ten small welded beams having similar welded details as the bridge beams. Details of the experiments are given elsewhere[3]).

The beams were fabricated from A 373 plate steel. The yield point of the beam flanges was 38,700 psi and the ultimate strength was 63,400 psi. The steel had 0.18—0.23% Carbon, 0.53—0.94% Manganese, 0.007—0.023% Phosphorus and 0.019—0.030% Sulfur. These properties were similar to those of the beams in the Road Test bridges.

All beams were 12-in. deep and 11-ft. long I-beams. Six specimens were built up of two $^3/_4$-in. thick flanges welded to a $^3/_{16}$-in. web; $^1/_2$-in. thick cover plates were attached to both the tension and the compression flanges with $^1/_4$-in. fillet welds. Four specimens were built up of two $^3/_8$-in. thick flanges welded to a $^1/_4$-in. web and a $^1/_4$-in. thick cover plate attached to the tension flange with $^3/_{16}$-in. fillet welds. The welding was done manually with low hydrogen electrodes conforming to AWS Specification E-7016.

---

[3]) Munse, W. H., and Stallmeyer, J. E.: "Fatigue in Welded Beams and Girders", *Highway Research Board*, Bulletin 315, 1962.

The specimens were tested in flexure on a span of 8 ft. 6 in. in an Illinois walking beam fatigue testing machine. The load was applied at a rate of 180 cycles per minute as two concentrated loads located 6 in. each side of midspan.

Test Results

Bridge Structures

The stresses caused by dead loads and by regular test traffic at the critical sections in the bridge beams are summarized in Table I. The minimum stress was obtained as the difference between the dead load stress and the rebound stress (Fig. 1). The dead load stresses were calculated with actual weights of the materials and were checked by strain measurements on several bridges. The stress range was obtained as the sum of the maximum live load and impact stress and the rebound stress (Fig. 1).

The stress range varied from one passage of the test vehicle to another as is shown by the standard deviations in Table 1. However, the variations in the stress range were smaller than one would expect to find under mixed traffic on bridges in the highway system.

Fatigue cracks were first discovered late during the period of the regular test traffic. The number of vehicle trips at the time the cracks were found is listed in the last column of Table 1. The fatigue cracks first appeared in the bottom surface of the rolled section at the toe of the welds connecting the cover plate and were usually $^1/_4$ to $^1/_2$ in. long. The cracks were determined by visual inspection of the critical areas with a magnifying glass.

Except for the crack at the approach end of the plate on the interior beam of Bridge 2 B, the cracks changed either very little or not at all during the remainder of the traffic. The one crack on Bridge 2 B spread through one quarter of the bottom flange as shown in Fig. 2. By the end of regular test traffic Bridges 1 A, 2 B and 3 B were subjected to approximately 556,000 vehicle trips. Bridge 1 A had ten fatigue cracks, Bridge 2 B had five cracks and Bridge 3 B had two cracks at that time. Two fatigue cracks were found on Bridge 9 A and one on Bridge 9 B: these two bridges were subjected to approximately 478,000 vehicle trips.

The number of stress cycles, N, at first detection of fatigue cracks varied from 478,000 to 606,000. The corresponding $\log N$ was 5.679 to 5.783. Hence, the total variation in the logarithmic life was only 1.8%. Because of the small variation on the logarithmic life, the regression line in Fig. 3, including all test data, can be considered as corresponding to the average $\log N$ or 530,000 stress cycles.

It can be seen from Fig. 3 that an increase in the minimum stress from 5,000 to 20,000 psi caused no change in the number of cycles to fatigue cracking

Table 1. Fatigue Strength of Steel Bridges

Bridge	Beam	Critical Section	Min. Stress ksi	Stress Range		Cycles to Cracking
				Mean ksi	Std. Dev. ksi	
1 A	Interior	Approach	10.7	13.3	1.20	556,900
	Center	Approach	13.8	13.6	0.92	536,000
	Exterior	Approach	16.5	12.8	0.94	536,000
	Interior	Exit	10.5	15.5	1.17	557,300
	Center	Exit	13.6	15.7	0.98	536,000
	Exterior	Exit	16.1	15.1	1.04	536,000
2 B	Interior	Approach	14.0	15.9	1.75	531,500
	Center	Approach	18.0	15.8	1.74	531,500
	Exterior	Approach	21.1	15.2	1.80	606,000
	Center	Exit	18.0	15.4	1.39	531,500
3 B	Center	Approach	15.0	14.0	2.08	535,500
	Exterior	Exit	17.9	13.4	1.59	557,800
9 A	Exterior	Approach	9.4	16.1	1.44	477,900
	Exterior	Exit	9.2	16.4	0.21	477,900
9 B	Center	Approach	6.7	17.6	1.40	477,900

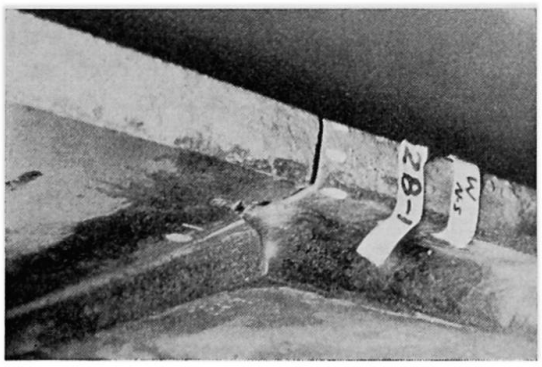

Fig. 2. Propagation of fatigue crack.

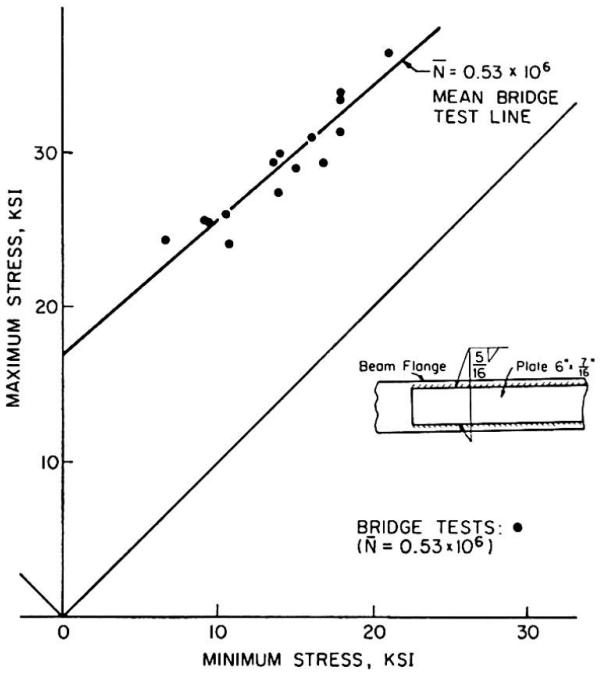

Fig. 3. Results of bridge tests.

when accompanied by a decrease in the stress range from 16,500 to 14,500 psi. Apparently a large change of the minimum stress accompanied by no change in the stress range may be expected to produce only a small change in the

number of cycles to fatigue cracking. In other words, the minimum stress appeared to have only a small effect on the fatigue life.

Laboratory Beams

The results of the laboratory fatigue tests of beams with partial-length cover plates are given in Table 2. Six beams were tested at the minimum stress of 400 psi and four were tested at the minimum stress of 15,400 psi. The maximum stress was so chosen that one-half of the specimens, at each level of minimum stress, failed above 1,000,000 cycles and the other half below 400,000 cycles. All fatigue cracks started at the toe of the longitudinal weld connecting the cover plate and propagated transversely and vertically through the beam flange.

Table 2. Laboratory Fatigue Tests of Beams

Test Specimen	Minimum Stress, ksi	Maximum Stress, ksi	No. of Cycles To Failure	No. of Cycles To Last Inspection Prior to Failure
CPDF-1	0.4	13.2	1,431,500	1,000,100*)
CPDG-1	0.4	13.3	2,819,300	2,308,500**)
CPCD-1	0.4	14.3	1,308,600	1,126,400
CPDF-2	0.4	23.9	291,800	220,700
CPAD-1	0.4	24.9	256,700	160,800
CPCD-2	0.4	26.0	260,200	241,600**)
1	15.6	28.0	1,378,400	1,312,800
4	15.4	27.7	1,524,500	1,150,900
2	15.4	36.0	350,200	307,400
3	15.4	36.7	285,200	222,100

*) Specimen had a crack 1 ½ in. long.
**) Specimen had a crack ¼ in. long.

The number of cycles at which the crack became visible in the laboratory specimens was not determined. However, at the last inspection prior to failure small cracks, $^1/_4$ to $1\,^1/_2$ in. long, were found in three beams while no cracks were found in the remaining seven beams. Apparently, had the inspections been more frequent, cracks in the seven specimens would have been found somewhere between the "last inspection" and the "failure".

The number of cycles to last inspection is listed in Table 2 in addition to the number of cycles to failure. As all last inspections were made relatively close to failure, the number of cycles to last inspection will be considered as the number of cycles to fatigue cracking.

Analysis of Test Results

Laboratory Tests

The experimental data from Table 2 are plotted in Fig. 4 in which the stress range is given as a function of the logarithm of the number of cycles to cracking. A separate plot is included for each minimum stress level.

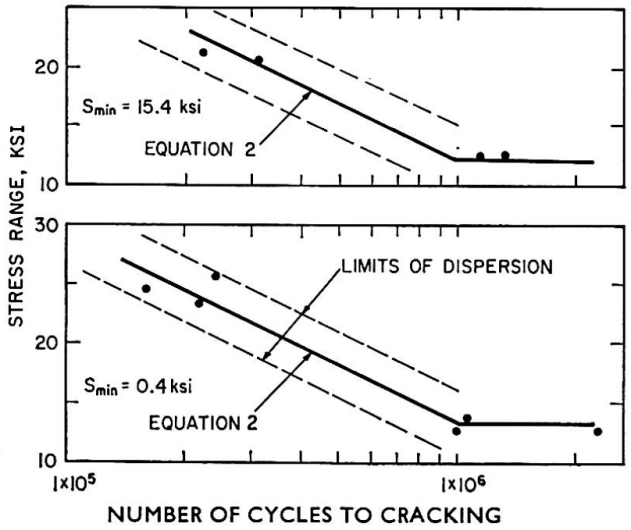

Fig. 4. S-N diagrams of laboratory data.

The relationship between the stress range and the logarithm of the number of cycles to failure was assumed to be represented by two straight lines: a sloping line up to 1,000,000 cycles (fatigue strength) and a horizontal line beyond 1,000,000 cycles (endurance limit).

The sloping line was expressed by the following mathematical model:

$$\log N = A + B\,S_r + C\,S_{min} \pm E, \tag{1}$$

in which

S_r = $S_{max} - S_{min}$; range of stress, ksi
S_{min} = minimum stress, ksi
S_{max} = maximum stress, ksi
N = number of cycles to failure
A, B, C = empirical constants
E = estimate of experimental error

Coefficients A, B, and C of Eq. 1 were evaluated by regression analysis of the laboratory data.

The analysis was based on the number of cycles to the last inspection before failure. For specimens with N larger than 1,000,000, the value of $\log N = 6.0$ was used in the analysis. The following equation was obtained for the number of cycles to fatigue cracking:

$$\log N = 6.827 - 0.0620\,S_r - 0.0056\,S_{min} \pm 0.180. \tag{2}$$

The error term at the end of the equation is equal to twice the standard error of estimate.

Equation 2 applies only up to 1,000,000 cycles. The stress range corresponding to cracking at 1,000,000 cycles represents the endurance limit. Both Eq. 2 and the endurance limit are shown in Fig. 4.

An examination of the coefficients of Eq. 2 reveals the relative significance of the stress range and the minimum stress. For example, a decrease in the stress range of 10 ksi increases the logarithmic life by 0.62; but the same decrease in the minimum stress increases the logarithmic life only by 0.056 or less than one-tenth as much as the change in the stress range. The relatively small effect of the minimum stress on fatigue life is illustrated in Fig. 5 containing the two mean regression lines for the laboratory tests and the limits of dispersion.

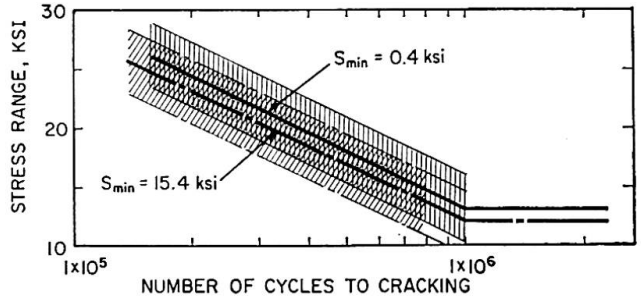

Fig. 5. Effect of minimum stress on fatigue life.

Comparison of Laboratory and Bridge Tests

Fatigue cracking of the bridge beams furnished data for quantitative comparisons with the results of the simpler laboratory tests.

In the laboratory tests the stress fluctuations followed a simple sine wave; in the bridge tests the shape of the time-stress curve was irregular including major stress waves caused by the weight of the moving vehicles, minor stress waves caused by vibration of the bridge, and rest periods corresponding to the intervals between the trucks and to periodic breaks in the test traffic. Finally, in the laboratory tests the duration of one stress cycle was of the order of one second or less while in the bridge tests the intervals of the major stress cycles were of the order of 40 seconds or more. Thus the stress histories of the bridge tests differed considerably from those of the laboratory tests.

In comparing quantitatively the results of the bridge tests with laboratory data, the only characteristics of the stress histories considered were the minimum stress and the stress range. The effects of the speed of loading, rest periods, and vibrations were disregarded because of lack of methods which would permit their inclusion in the analysis.

The results of the individual comparisons are shown in Fig. 6 in which the ratio of the observed to the computed number of cycles to fatigue cracking is plotted for every beam section with a fatigue crack detected during the traffic period. The individual comparisons are plotted corresponding to the sequential

listing of the observed number of cycles to cracking in Table 1. The computed values were obtained by three methods: the bars in Fig. 6, each representing one beam cross-section, show the results for all three methods.

The method designated as "Miner's Hypothesis" accounted for the variations in the stress range with the aid of Miner's Hypothesis of cumulative damage[4]). In this analysis, use was made of the minimum stress and both the mean and the standard deviation of the stress range (Table 1). Details of this method may be found elsewhere[2]).

The method designated in Fig. 6 as "Mean Stress Range" neglected the variations in the stress range. Values of N were calculated from Eq. 2, neglecting the error term, with the minimum stress and the mean stress range.

Finally, the method designated as "Rebound Neglected" used the same approach as the method "Mean Stress Range" except that the minimum stress was taken equal to the dead load stress and the stress range was taken as the live load and impact stress. In other words, the rebound stress (Fig. 1) was neglected in the computations.

Fig. 6 includes also the limits of dispersion of the test data computed from the error term in Eq. 2. It will be noted that all but two ratios based on Miner's Hypothesis and on Mean Stress Range fall within these limits. Furthermore, the values calculated with the aid of Miner's Hypothesis were in the best agreement with the laboratory data. Finally, the data in Fig. 6 demonstrate the need to consider the rebound stress in the analysis.

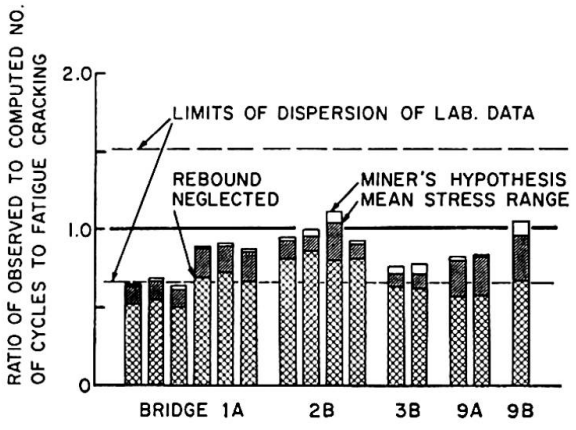

Fig. 6. Comparison of individual bridge test results with laboratory data.

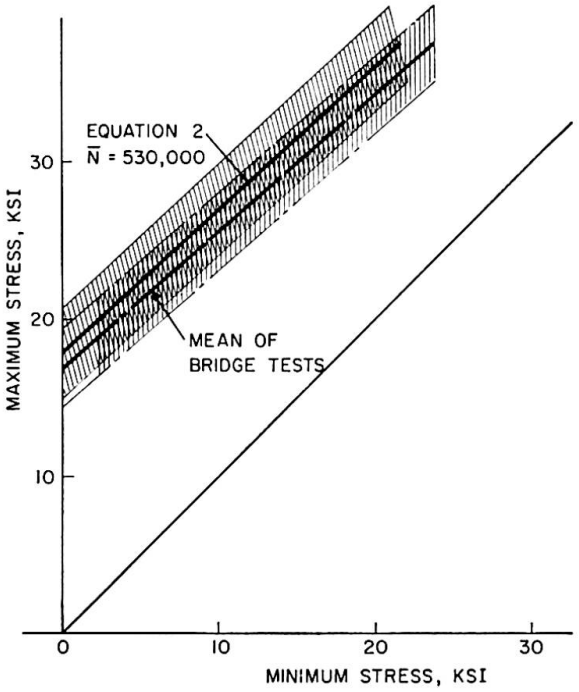

Fig. 7. Overall comparison of bridge and laboratory tests.

4) Miner, M. A.: "Cumulative Damage in Fatigue", *Journal of Applied Mechanics*, September, 1945.

The results of the overall comparisons are shown in Fig. 7. The regression line for the bridge tests is compared with a line computed from Eq. 2 for 530,000 cycles. The means as well as the limits of dispersion, equal to twice the standard error of estimate, are included for both the bridge tests and the laboratory data. The scatter bands for the two series of tests show a substantial overlap.

The comparisons in Fig. 6 and 7 show that the results of the bridge tests were in excellent agreement with the results of the simple laboratory fatigue tests. However, the bridge beams appeared to be slightly weaker in fatigue than the laboratory specimens. Fortunately, the differences were too small to be of practical engineering significance.

The comparisons show further that it should be satisfactory to base the engineering analysis of the fatigue strength of structures solely on the magnitude of the minimum stress and the stress range. Of the two, the effect of the stress range appears to be considerably more important and therefore should be estimated with greater accuracy: it should include not only the live load and the impact stresses but also the rebound stress. Furthermore, for structures with large variations of the stress range it may be necessary to consider the effects of the so-called cumulative damage.

Comparison of Test Results with Design Specifications

It has been shown in the preceding discussion that the fatigue strength of beams with partial-length cover plates is satisfactorily represented by Eq. 2. Thus the equation may be used to examine the design stresses permitted for such members by current design specifications. As all test beams were made of structural grade steel, the comparisons are limited to such steels.

Fig. 8 shows allowable stresses for 2,000,000 cycles used in Great Britain (steel BS 15)[5], U.S.A. (A 36)[6], U.S.S.R. (ST 3)[7] and West Germany (ST 37)[8]. The figure includes also the mean fatigue strength and the limits of dispersion of test data for 2,000,000 cycles.

The allowable stresses are represented by a sloping line (or a series of sloping lines) and a horizontal line. Except for the allowable stresses specified by the American Welding Society, there is little variation between the allowable stresses. The sloping lines fall slightly below and follow reasonably well the slope of the mean fatigue strength. However, they are within the scatter band of the test data.

---

[5]) British Standard 153: 1958, "Steel Girder Bridges" (with Amendments 1, 2, 3 and 4), 1962.

[6]) American Welding Society, "Specification for Welded Highway and Railway Bridges", 1963.

[7]) TUPIN-SV-55, "Specification for the Design and Construction of Welded Railway Bridges", 1955.

[8]) DV 848, "Regulations for Welded Railway Bridges", 1955.

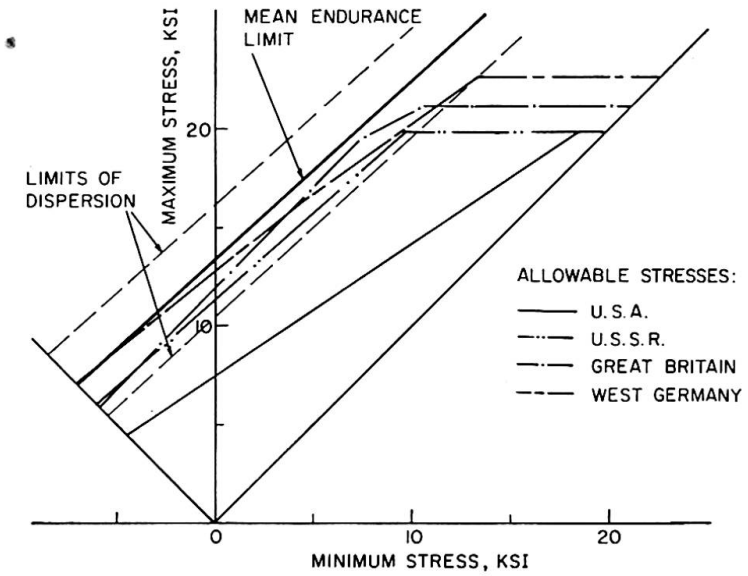

Fig. 8. Fatigue strength and allowable stresses for 2,000,000 cycles.

The horizontal lines represent the limitation imposed by the basic design stress, a condition independent of fatigue considerations. For the four mild steels considered, the basic design stress varied from 20 to 22.7 ksi.

The allowable stresses specified by the American Welding Society are considerably more conservative. While the factor of safety may be considered satisfactory for the case of full stress reversal, the divergence of the sloping line from the mean fatigue strength results in a prohibitively large factor of safety.

Generalized Design Approach

Current design rules specify the allowable stresses for fatigue loading in terms of maximum and minimum stress. Separate sets of values are usually given for different weld details, different desired lives of the structure and different grades of steel. Studies carried out in conjunction with the tests reported here indicate that this seemingly endless procession of design equations may be replaced by a single formula based on classic concepts of fatigue strength and a different set of two empirical coefficients for each different category of weld details.

Several investigators have reported that the fatigue lives of beams of different steels, having the same type splice configuration, were approximately the same[9]). Recently GURNEY[10]) concluded on the basis of an extensive

[9]) GURNEY, T. R.: "Fatigue Strength of Fillet Welded Joints in Steel", *British Welding Journal*, March 1960; STALLMEYER, J. E., NORDMARK, G. E., MUNSE, W. H., NEWMARK, N. M.: "Fatigue Strength of Welds in Low Alloy Structural Steels", *Welding Journal*, Vol. 35, January 1956.

[10]) GURNEY, T. R.: "Fatigue Tests of Butt and Fillet Welded Joints in Mild and High Tensile Structural Steels", *British Welding Journal*, November 1962.

investigation that the fatigue strength of *similar welded details* in mild steel and high tensile steel can be represented by the same S-N curve. This point is illustrated in Fig. 9 presenting the results of fatigue tests of tension joints with transverse butt welds in mild (BS 15 and A 7, $Fy = 35{,}000$ psi)[9],[10]) low-alloy (BS 968 and A 242, $Fy = 54{,}000$ psi)[9],[10]) and constructional alloy (N-A XTRA 100, $Fy = 93{,}000$ psi)[11]) steels. The principal difference among the different grades of steel is the point at which the curve starts to deviate appreciably from the straight line. As this point of departure is generally above the yield point of the material, it is only of academic interest.

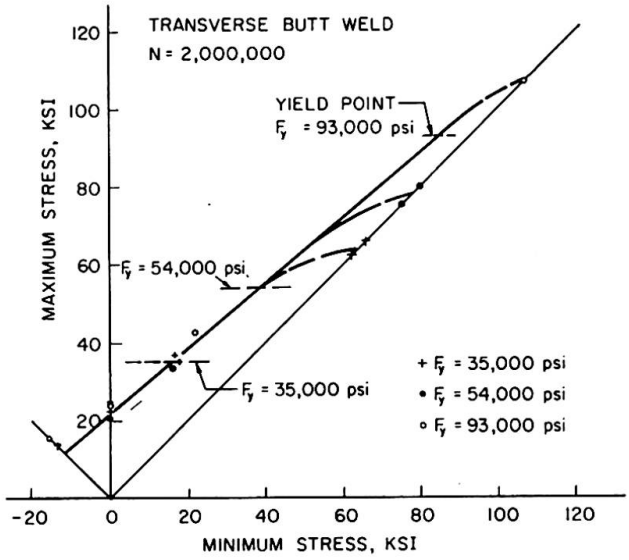

Fig. 9. Effect of steel strength on fatigue strength of welded joints.

Therefore, the same sloping line representing a specific fatigue life is applicable to all steels irrespective of their yield point or ultimate strength. This sloping line can be represented by a general design formula. The horizontal cut-offs will be different for various steels since they are usually determined by applying a uniform factor of safety against the static strength of the material. This consideration is independent of the fatigue strength.

The general design formula for fatigue strength may be expressed in several different terms[12]) but for the purposes of this discussion the following form

---

[11]) Scott, G. R., Stallmeyer, J. E., and Munse, W. H.: "Fatigue Strength of Transverse Butt-Welded Joints in N-A XTRA 100 Steel", University of Illinois, 1963.

[12]) For example, one of the better known variations of this formula is:

$$S_{max} = \frac{\alpha}{1 - \beta k},$$

where $k = S_{min}/S_{max}$ and the symbols "α" and "β" are empirical coefficients.

was chosen:

$$S_r = C_1 - (1 - C_2)\, S_{min}, \tag{3}$$

S_r = permissible stress range
S_{max} = maximum stress
S_{min} = minimum stress
C_1 = maximum permissible stress for a 0 to tension loading and N cycles
C_2 = slope of the permissible stress line

Empirical coefficients C_1 and C_2 must be evaluated for each category of weld details. This may be done by a statistical analysis of the test data using the relationship given by Eq. 1. The coefficients C_1 and C_2 may then be evaluated as:

$$C_1 = \frac{\log N - A'}{B}, \tag{4}$$

$$C_2 = \frac{B - C}{B}, \tag{5}$$

where A' is the empirical constant A (Eq. 1) corrected for the error term (or its multiple). *The correction for the error term decreases the probability of fatigue failure and thus provides the necessary factor of safety.*

An item of particular interest is the magnitude of coefficient C_2: its value is often close to 1.0. For example, for beams with partial-length cover plates (Eq. 2) it is equal to 0.91. The substitution of $C_2 = 1.0$ in Eq. 3 provides an approximate rule for guarding against fatigue failure: the stress range must not exceed a certain allowable value which depends only on the category of weld detail and the desired life of the structure.

Summary

Tests of five slab and beam steel bridges with partial-length cover plates are discussed. All bridges were subjected to 480,000 or 560,000 passages of test trucks. The number of stress cycles at fatigue cracking of steel bridge beams are compared with laboratory fatigue data.

Four current specification requirements for design against fatigue are compared with the results of these tests, and a generalized approach to the problem of fatigue design is outlined.

Résumé

Les auteurs analysent les résultats d'essais exécutés sur cinq ponts, constitués d'une dalle reposant sur des poutres métalliques renforcées par des semelles sur une partie de leur longueur. Tous les ponts ont été sollicités par

le passage de 480.000 ou 560.000 camions. On compare les essais sur ponts et ceux au laboratoire en considérant le nombre de cycles précédant la formation de fissures dues à la fatigue.

On compare également les résultats de ces essais aux sollicitations admissibles à la fatigue fixées par quatre règlements; on expose en outre, dans ses grandes lignes, une méthode généralisée de calcul de la résistance à la fatigue.

Zusammenfassung

In diesem Beitrag werden an fünf Brücken mit stählernen Hauptträgern, gebildet aus durch aufgeschweißte Gurtplatten teilweise verstärkten I-Walzprofilen und einer Stahlbeton-Fahrbahnplatte, durchgeführte Versuche besprochen. Alle Brücken werden entweder 480 000 oder 560 000 Überfahrten von Testlastenzügen unterworfen. Die Lastwechselzahlen für das Auftreten von Ermüdungsrissen an den Stahlträgern werden mit den Werkstattergebnissen verglichen.

Vier zur Zeit geltende Dauerfestigkeitsvorschriften werden den Ergebnissen dieser Versuche gegenübergestellt und anschließend wird eine allgemeine Näherungslösung für den Dauerfestigkeitsnachweis gegeben.

IId2

Life Estimate of Fatigue Sensitive Structures

Estimation de la durée de service d'ouvrages sensibles à la fatigue

Lebensdauer von ermüdungsempfindlichen Tragwerken

A. M. FREUDENTHAL
Columbia University, New York

1. Introduction

Metal structures subject to a large number of repeated loads of statistically variable intensity S may fail in either of two modes:

a) By excessive deformation, instability or sudden fracture resulting from the single occurrence of an unexpectedly high rare load intensity.
b) By progressive damage produced by repeated loads of operational intensity, in the form of distributed micro-cracks coalescing into localized macro-cracks, terminated by the occurrence of a load of high, but not unexpected intensity by which the damaged structure is destroyed.

While the first mode is usually referred to as "ultimate load failure" and the second as "fatigue failure", the latter is, in essence, also an ultimate load failure but one involving the fatigue-damaged structure, and therefore occurring under a terminal load of considerably lower intensity and of much higher frequency of occurrence than the "ultimate load" producing failure in mode a).

In this differentiation it is implied that the spectrum of operational loads which produce fatigue damage differs from the spectrum of "ultimate loads" which produces both the ultimate load and the fatigue failure in such a way that the latter cannot be obtained from the former by simple extrapolation towards very low probabilities of occurrence. In essence the spectrum of ultimate loads could however be considered as a spectrum of extreme values of large samples of operational loads. By this assumption a quantitative relation between the two load spectra could be established.

It should be noted that this concept of "fatigue failure" only applies to repeated *variable* load intensities. If a constant load intensity is repeated, as in a conventional fatigue test, fatigue failure occurs when the progressive damage in $(N-1)$ load repetitions has reduced the resisting section to such an extent that it can no longer carry the load at its N^{th} repetition. In this case the statistical variation of the load intensity, which produces the formal similarity between ultimate-load- and fatigue-failures, vanishes as a design

parameter and the statistical variation of the fatigue life is due entirely to the variation in the rate of progressive damage $\left(\frac{dD}{dn}\right)$ resulting from the "inhomogeneity" of the polycrystalline structure of the metal. It is assumed that this rate of damage per load cycle is proportional to the difference between the applied stress level and a "threshold stress" (endurance limit); under constant load intensity S the effective stress increases as the initial cross section A is reduced by progressive damage to $(A - A_r)$. Introducing $D = \left(1 - \frac{A_r}{A}\right)$, the stress increases therefore as $(1-D)^{-k}$, where $0 < D < 1$ is a measure of fatigue damage and $1 < k < 2$ characterizes the effect of the reduced cross section on the resultant stress intensity. The damage rate can therefore be expressed by

$$\frac{dD}{dn} = f\left[\frac{S}{(1-D)^k}\right]. \tag{1}$$

2. Return Period of Ultimate Load Failure

The life estimate of structures failing in mode a) can be based on the evaluation of the "return period" of ultimate failure. Since the probability of such failure P_U is related to the safety factor ν considered as the quotient of two statistical variables [1]

$$\nu_U = \frac{R}{S}, \tag{2}$$

where R is the structural resistance under ultimate load conditions with distribution $P_1(R)$, and S the "ultimate load" with distribution $P_2(S)$, by the assumption that

$$P_U = \int_0^{\nu_U} p(\nu_U)\, d\nu_U = P(\nu_U) \quad \text{for} \quad \nu_U = 1 \tag{3}$$

the mean "return period" of ultimate failure

$$\overline{T}_U = P_U^{-1} \tag{4}$$

expresses the mean number of repetitions of the statistical load S required, on the average, to produce one failure in nominally identical structures of statistical resistance R. The probability distribution of the return period, which expresses the probability that failure will occur before T_U load repetitions

$$P(T_U) = 1 - (1 - P_U)^{T_U} \tag{5}$$

since $(1-P_U)^{T_U}$ is the probability that failure will not occur in T_U load repetitions. If P_U is small and T_U is large Eq. (5) may be written

$$P(T_U) = 1 - \exp\left(-\frac{T_U}{\overline{T}_U}\right). \tag{6}$$

Hence the probability that failure with mean return period $\bar{T}_U$ will not occur before T_U load repetitions, which is the probability of survival

$$L(T_U) = [1 - P(T_U)] = \exp\left(-\frac{T_U}{\bar{T}_U}\right) \tag{7}$$

or, for small $P(T_U)$

$$P(T_U) = \frac{T_U}{\bar{T}_U}. \tag{7a}$$

If the structure is to survive the "mean return period" of ultimate failure with a probability $[1 - P(T_U)]$ the return period of failure to be used for design is

$$\bar{T}_{UD} \sim \frac{T_U}{P(T_U)} = [P_U\, P(T_U)]^{-1}. \tag{8}$$

In other words if the structure shall survive a specified return period of failure with a specified probability of $[1 - P(T_U)]$, its design return period $\bar{T}_{UD}$ should be associated with a safety factor that ensures a probability of failure of $[P_U\, P(T_U)] \ll P_U$. Hence the "risk of ultimate failure" r_U, which is the probability of ultimate failure of a structure that has survived T_U load repetitions

$$r_U = \frac{p(T_U)}{L(T_U)} = -\frac{d\,L(T_U)}{L(T_U)} = -\frac{d}{d\,T_U} ln\, L(T_U) = \bar{T}_U^{-1}$$

is constant. If the structure is designed for a return period of ultimate failure $\bar{T}_{UD} \gg \bar{T}_U$, the risk of failure is reduced by the factor of $[P(T_U)]^{-1}$.

3. Return Period of Fatigue Failure

While practically all metal structures subject to repeated loads will show fatigue damage if the number of repetitions is large enough, fatigue is a significant design criterion only if the "return period" of fatigue failure under repeated variable load intensity is considerably shorter than the return period of ultimate failure. The safety factor of a structure subject to fatigue damage is no longer a stationary statistical variable but decreases with increasing number n of load repetitions which gradually reduce the resistance R to ultimate load failure. Hence, instead of Eq. (2) where ν_U is independent of n, ν is now a function of n

$$\nu_F = R(n)/S = \nu(n) \tag{9}$$

through the fatigue damage $D(n)$ which expresses the reduction of the resistance R by changing the distribution $P_1(R)$ to a family of distributions

$$P_1[R(n)] = P_1[R[1 - D(n)]^k], \tag{10}$$

where $D(0) < D \leqq D(n)$, with $D(0) = 0$ and $D(n) = 1$.

The distribution of

$$\frac{R}{S}[1 - D(n)[^k = \nu_U [1 - D(n)]^k \tag{11}$$

necessarily differs from the distribution of the quotient (R/S) because $[1 - D(n)]^k$ is not a constant but a statistical variable due to the statistical character of the damage function $D(n)$. Only if the distributions of both ν_U and $[1 - D(n)]^k$ are logarithmic-normal, the distribution of ν_F is also logarithmic-normal.

Under the simplifying assumption of non-statistical linear damage accumulation $D(n)$ the resulting relation between the distribution functions

$$P(\nu_U) = P\left[\frac{\nu_F}{[1 - D(n)]^k}\right] \tag{12}$$

implies that the probability of fatigue failure P_F at which $\nu_F \leqq 1$, is at the abscissa of the function $P(\nu_U)$ at which $\nu_U \leqq [1 - D(n)]^{-k}$. Thus the distribution functions $P(\nu_U)$ computed under various assumptions [2] for the distribution functions $P_1(R)$ and $P_2(S)$ and for the "central safety factor" of the design $\nu_{U0} = R_0/S_0$, can be used to determine the probability of fatigue failure under the ultimate load spectrum S as a function $P_F[D(n)]$ of prior fatigue damage produced by the operational load spectrum. Since $[1 - D(n)]^{-k} > 1$, the probabilities $P_F > P_U$.

Thus, for instance, for logarithmic-normal distributions $P_1(R)$ and $P_2(S)$ with $\nu_{U_0} = (\breve{R}/\breve{S})$ being the ratio between the median values of R and S, the probability function

$$P(\nu_U) = \Phi\left[\frac{1}{\delta}\log\left(\frac{\nu_U}{\nu_{U_0}}\right)\right], \tag{13}$$

where the error integral

$$\Phi(t) = \int_{-\infty}^{t} \frac{1}{\sqrt{2\pi}} \exp\left(-\frac{1}{2}t^2\right) dt \tag{14}$$

and the resulting standard deviation

$$\delta = [\sigma(\log R) + \sigma(\log) S)]^{1/2}. \tag{15}$$

The probability of fatigue failure therefore according to Eqs. (12) and (11)

$$P_F = P\{[1 - D(n)]^{-k}\} = \Phi\left\{\frac{1}{\delta}\log[(1 - D)^{-k}(\nu_{U_0})^{-1}]\right\} = \Phi\left[\frac{1}{\delta}\log\left(\frac{1}{\nu_{F_0}}\right)\right]. \tag{16}$$

Since $\nu_{F_0} = [1 - D(n)]^k \nu_{U_0}$ is a function of $D(n)$, the probability of fatigue failure P_F become functions of the damage D, and thus functions of the number n of load cycles applied.

Using the diagram $P(\nu)$ computed [2] for logarithmic-normal distributions of R and S with $\sigma_s/\breve{S} = 0.30$ and $\sigma_R/\breve{R} = 0.10$ for various ultimate load design values ν_{U_0} between 1.0 and 4.5 (Fig. 1) the following approximate values are

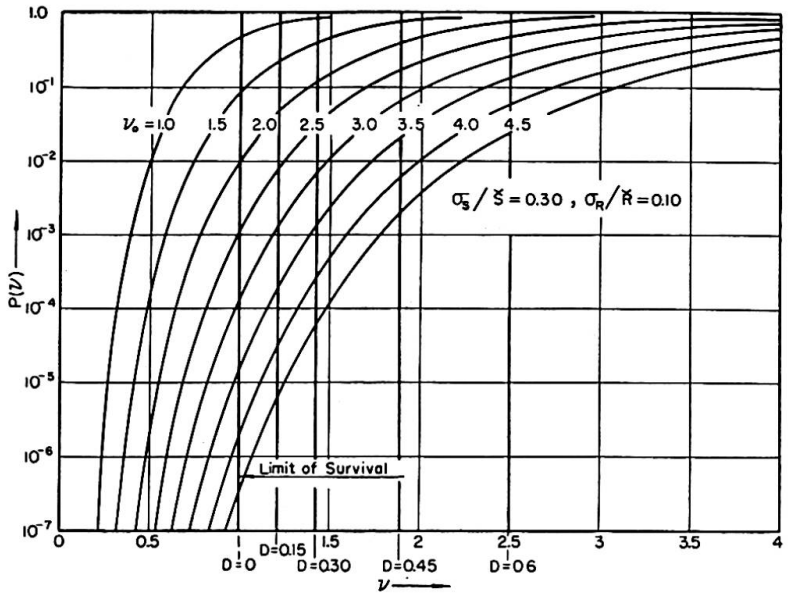

Fig. 1.

obtained for P_F as a function of D for the ultimate load design safety factors $\nu_{U_0} = 2$, 3 and 4:

Table I

D		0.0	0.15	0.30	0.45	0.60
P_F	$\nu_0 = 2$	10^{-2}	5×10^{-2}	10^{-1}	5×10^{-1}	9×10^{-1}
	$= 3$	2×10^{-4}	10^{-3}	8×10^{-3}	8×10^{-2}	3×10^{-1}
	$= 4$	3×10^{-6}	3×10^{-5}	3×10^{-4}	8×10^{-3}	8×10^{-2}

For the relation of D and the total number $n = \sum_i n_i$ of load cycles at the different stress levels S_i different assumptions can be made; the simplest is that of quasi-linear damage accumulation with stress interaction factors ω_i to compensate for the damaging ($\omega_i > 1$) or strengthening ($\omega_i < 1$) effect of interaction between high and low stress intensities [3] and with minimum lives N_{0i} delimiting the ranges of crack initiation and crack propagation [4]

$$D = \sum_i \left(\omega_i \frac{n_i - N_{0i}}{N_i - N_{0i}} \right) \quad \text{for} \quad N_{0i} < n_i < N_i . \tag{16}$$

For $n_i < N_{0i}$, $D = 0$.

With the aid of Eqs. (16) and (12) the relation between P_F and n can be established: with increasing value of damage D the probability of failure increases rapidly, as illustrated by Table I, and the mean return period of failure $\overline{T}_F$

$$\overline{T}_F(n) = [P_F(n)]^{-1} \tag{17}$$

decrease accordingly. Thus there is a mean return period of fatigue failure $\overline{T}_F[D(n)] = \overline{T}_F(n)$ associated with each damage level $D(n)$, and the ratio

$$\frac{P_F(n)}{P_U} = \frac{\overline{T}_U}{\overline{T}_F(n)} = f(n) > 1 \tag{18}$$

can be considered as a "fatigue sensitivity" factor of the structure. Obviously, the fatigue sensitivity increases with increasing damage, but for the same amount of damage also with increasing design safety factor for ultimate load design. This can be illustrated by converting Table I into a table of "fatigue sensitivity" factors f, dividing all rows by the value P_U which is identical with P_F for $D=0$

Table II

D		0.0	0.15	0.30	0.45	0.60
$f(D)$	$\nu_0 = 2$	1	5	10	50	90
	$= 3$	1	5	40	400	1500
	$= 4$	1	10	100	2670	26700

The return period of fatigue failure at constant damage has a distribution similar to that of ultimate load failure according to Eq. (6):

$$P(T_F) = 1 - \exp(-T_F/\overline{T}_F) \tag{19}$$

or

$$L(T_F) = \exp(-T_F/\overline{T}_F) \tag{20}$$

and therefore the "design return period" of fatigue failure will depend on the selected probability of surviving the mean return period, which might be considered as the specified design life of the structure.

The value of $\overline{T}_F$ depends strongly on the damage function $D(n)$ which, in turn, is strongly affected by the "minimum fatigue life" $N_{0i} = N_0(S_i)$, which delimits the fatigue initiation period. Since the length of the fatigue initiation period in relation to the total fatigue life at constant stress or variable stress is a characteristic of the structural material as well as of residual stress fields in the fatigue-critical parts of the structure produced by previous load history or arbitrary prestraining [5], both effects can be introduced into the damage factor and thus into the estimate of the probability of fatigue failure under the relevant spectra of operational and "ultimate loads".

References

1. ALFRED M. FREUDENTHAL: "Methods of Safety Analysis of Highway Bridges." Preliminary Publication Sixth Congress IABSE, Stockholm 1960, pp. 656—664.
2. ALFRED M. FREUDENTHAL: «Die Sicherheit der Baukonstruktionen.» Acta Technica, Acad. Sc. Hung., Budapest 1964 (in print).
3. ALFRED M. FREUDENTHAL and R. A. HELLER: "On Stress Interaction in Fatigue and a Cumulative Damage Rule." J. Aerospace Sc., Vol. 26 (1959), pp. 431—442.

4. ALFRED M. FREUDENTHAL and E. J. GUMBEL: "Minimum Life in Fatigue." J. Am. Statist. Ass., Vol. 49 (1954), pp. 575—597.
5. W. WEIBULL: "A Theory of Fatigue Crack Propagation in Sheet Specimens." Acta Metallurgica, Vol. 2 (1963), p. 751.

Summary

By defining fatigue failure as an "ultimate load failure" of a structure damaged in fatigue by operational loads, the estimate of fatigue life can be reduced to that of a "mean return period" of an ultimate load type of failure for which statistical methods of safety analysis have already been developed. By applying such methods in conjunction with a simple fatigue damage function the fatigue sensitivity of a structure can be evaluated in terms of the ratio of the return periods of fatigue failure and ultimate load failure.

Résumé

En considérant la rupture par fatigue comme la «ruine sous une charge limite» d'un ouvrage déjà fatigué par l'action des charges de service, on peut ramener l'estimation de la durée de service à celle du «nombre moyen de répétitions de charges données» relatif à un type de ruine sous une charge limite pour lequel on connaît des méthodes statistiques qui permettent le calcul de la sécurité. Si on applique ces méthodes en utilisant une fonction d'endommagement par fatigue mathématiquement simple, on pourra évaluer la sensibilité à la fatigue d'un ouvrage en fonction des nombres de répétitions des charges relatifs à la rupture par fatigue et à la ruine sous une charge limite.

Zusammenfassung

Durch die Definition des Ermüdungsbruches als einen «statischen» Bruch des durch Ermüdungsbeanspruchungen unter Betriebslasten geschädigten Tragwerkes kann die Abschätzung der Lebensdauer unter Ermüdungsbeanspruchungen zurückgeführt werden auf die Bestimmung einer mittleren «Rückkehrzeit» eines «statischen» Bruches, für welchen statistische Methoden der Sicherheitsberechnung bereits entwickelt wurden. Durch Anwendung dieser Methoden im Zusammenhang mit einer einfachen Ermüdungsschädigungsfunktion wird es möglich, die Ermüdungsempfindlichkeit eines Tragwerkes auszuwerten und als das Verhältnis der «Rückkehrzeiten» von Ermüdungsbruch und statischem Bruch darzustellen.

Leere Seite
Blank page
Page vide

IId3

Kabel mit hoher Ermüdungsfestigkeit für Hängebrücken

Suspension Bridge Cables with Higher Fatigue Strengths

Câbles à haute résistance à la fatigue pour ponts suspendus

FRITZ LEONHARDT
Stuttgart

1. Einleitung

Für Hängebrücken oder Schrägkabelbrücken werden in Deutschland vorzugsweise patentverschlossene Seile verwendet, die zur Verankerung mit Weißmetall in Seilköpfen vergossen werden (Fig. 1). In anderen Ländern verwendet man sogar normale, offene Drahtseile oder Litzenseile mit Seilköpfen, sofern nicht bei großen Spannweiten in den USA und England Paralleldrahtkabel aus dünnen Drähten gesponnen werden.

Die großen Brücken werden in zunehmendem Maße mit den in Deutschland entwickelten Leichtfahrbahnen (orthotrope Platte) gebaut. Das Eigengewicht wird daher immer leichter, während die Verkehrslasten zunehmen. Entsprechend wird die Schwingbreite der Spannungswechsel unter Verkehrslasten im Vergleich zur Grundspannung infolge Eigengewicht immer größer. Dies bedeutet, daß die Ermüdungsfestigkeit solcher Seile oder Kabel eine zunehmende Rolle spielt.

Nun ist es bekannt, daß die Seile an ihren Verankerungen mit Seilköpfen, insbesondere infolge der hohen Temperatur des Vergußmetalles, keine sehr

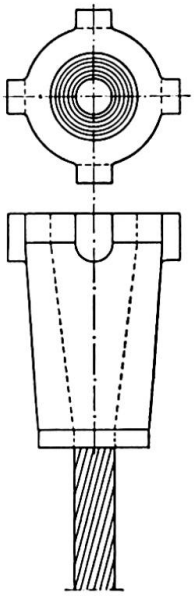

Fig. 1. Seilkopf als Seilanker.

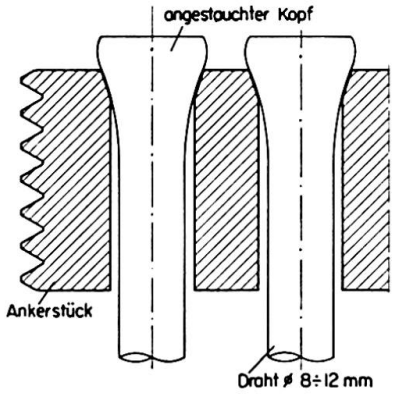

Fig. 2. Spezialkopfform der BBRV-Anker für Brückenkabel.

hohe Ermüdungsfestigkeit haben. Bei patentverschlossenen Seilen wurde selbst bei sorgfältiger Ausführung der Verankerung eine Schwingbreite von rund 1400 bis 1600 kp/cm² über einer unteren Grundspannung von 2500 kp/cm² bei einer mittleren Seilfestigkeit von 14 000 kp/cm² ermittelt [1]. Bei offenen Seilen liegt diese Schwingbreite noch niedriger.

Die paralleldrähtigen Kabel der Amerikaner mit schlaufenartiger Verankerung sind hinsichtlich ihrer Ermüdungsfestigkeit diesen Seilen mit Seilköpfen zweifellos überlegen. Sie haben jedoch andere Nachteile, so insbesondere die Notwendigkeit der Stoßmuffen und die mangelhafte und zeitraubende Ordnung der dünnen Drähte beim Herstellungsverfahren, die befürchten läßt, daß manche Drähte im Kabel sich kreuzen und beim hydraulischen Zusammenpressen mehr oder weniger abgequetscht werden.

2. Neue Kabelanker

Aufbauend auf den Erfahrungen, die beim Spannbeton gesammelt wurden, werden neuerdings Paralleldrahtkabel mit größeren Drahtdurchmessern, z. B. ∅ 8 bis ∅ 12 mm, aus kaltgezogenem, hochfestem Stahl hergestellt, die an ihren Enden mit einer speziellen BBRV-Verankerung versehen werden (Fig. 2)

Bei dieser im Spannbeton sehr bewährten Verankerungsart werden bekanntlich an den rechtwinklig abgeschnittenen Drahtenden Köpfchen kalt angestaucht, die sich gegen ein Ankerstück legen, wobei viele Drähte durch eng nebeneinander liegende Bohrungen hindurchgeführt werden. Das Ankerstück ist außen mit einem Gewinde versehen, das die Ankermutter bzw. den Stellring trägt, der die Kabelkraft auf die Ankerplatte überträgt (Fig. 3). Diese Anker brauchen weniger Platz als die Seilköpfe.

Während die Köpfchen bisher etwa Kugelform hatten, werden nunmehr auf Anregung des Verfassers die Köpfchen mit einem konischen Übergang angestaucht, so daß die Ankerkraft eine starke radiale Pressung in dem konischen Sitz des Ankerstückes hervorruft. Diese radiale Pressung hat zur Folge, daß das Köpfchen im Dauerschwingversuch nicht mehr abgeschert wird und daß eine Ermüdungsfestigkeit der Verankerung erreicht wird, die etwa der Ermüdungsfestigkeit des Drahtes selbst entspricht. Versuche an der EMPA, Zürich, haben gezeigt, daß man über einer unteren Spannung von rund 3500 kp/cm² eine Schwingbreite bis zu 2800 kp/cm² erreichen kann, also rund die doppelte Schwingbreite der im Seilkopf vergossenen Seile. Man kann damit in Brücken die Festigkeit dieser Drähte wieder voll ausnützen, während man bisher im Hinblick auf die schwingenden Beanspruchungen die obere maximale Spannung herabsetzen mußte. Mit dieser neuen Verankerungsart werden also wesentliche Vorteile für den Großbrückenbau erreicht.

Derartige Kabel können nun bis zu Längen von 40 oder 50 m genau so hergestellt werden wie Spannglieder für Spannbeton, indem man die parallelen

Drähte in Hüllrohren führt und sie nachträglich zum Schutz gegen Temperaturänderungen und Korrosion mit Zementmörtel auspreßt. Bei der Anwendung solcher Kabel für den Fußgängersteg über die Schillerstraße in Stuttgart [2] wurden Hüllrohre aus dem Kunststoff Hostalen (Polyäthylen) verwendet, wodurch ein haltbarer Schutz erzielt wurde.

3. Neue Herstellungsart der Kabel

Für größere Kabellängen, insbesondere für Kabel von Hängebrücken oder weitgespannten Schrägkabelbrücken wird eine neue Herstellungsart empfohlen, die der Verfasser schon 1941 aus Beobachtungen an einem Versuchsstück der Kabel für die San-Francisco-Bay-Brücke ableitete [3, 4]. Die Amerikaner legen bekanntlich etwa kreisrunde, gebändselte Drahtbündel mit je 60 bis 90 Stück 5-mm-Drähten zu dem ungefähr kreisrunden Kabel zusammen (Fig. 4a) und pressen dieses Kabel hydraulisch auf einen möglichst kleinen Querschnitt radial zusammen (Fig. 5), wonach das ganze Kabel mit Draht umwickelt wird.

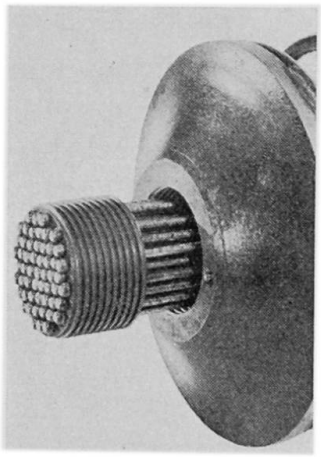

Fig. 3. BBRV-Anker für viele Drähte.

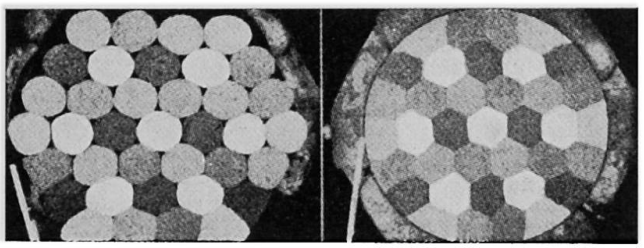

a) b)

Fig. 4.
a) Aus Drahtbündeln zusammengelegtes Kabel einer US-Hängebrücke vor dem Zusammenpressen.
b) Form der ursprünglich etwa kreisrunden Bündel des Bildes a) nach dem Pressen.

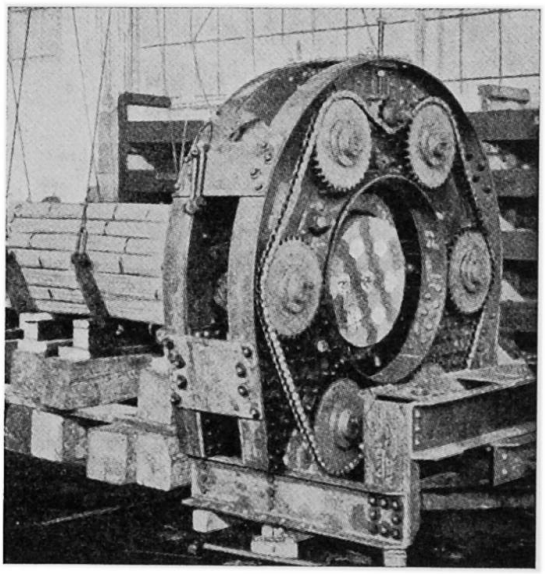

Fig. 5. Das Kabel wird mit großen hydraulischen Pressen radial auf Kreisquerschnitt gepreßt.

Der Versuch zeigte nun, daß beim Zusammenpressen die ursprünglich etwa kreisrunden Drahtbündel im inneren Bereich des Kabels sechseckig wurden (Fig. 4b). Dies ist ganz natürlich, weil Drähte in sechseckiger Anordnung jeweils das Hohlraum-Minimum ergeben. Es liegt nun nahe, die Drähte von vornherein in sechseckigen Bündeln anzuordnen (Fig. 6). Dies kann leicht geschehen, indem alle Drähte eines sechseckigen Bündels gleichzeitig von ihren Ringen abgezogen und durch Führungen auf die sechseckige Anordnung gebracht werden. Das Bündel läuft dabei zwischen sechs mit Gummi belegten Rollen hindurch, die die Drähte radial eng zusammenpressen. Unmittelbar dahinter wird das Bündel mit einem dünnen Draht bei verhältnismäßig großer Ganghöhe wendelartig umwickelt bzw. gebändselt. Das Bündel behält dann auch beim Transport seinen sechseckigen Querschnitt, selbst wenn es über Krümmungen hinweggeführt wird. Man kann ein solches Kabel mit ausreichend großem Krümmungsradius auch über gekrümmte Kabelsattel endgültig verlegen, weil schon geringe Unterschiede der Längsspannungen die verschiedene Drahtlänge im Krümmungsbereich ausgleichen, zudem sich die Drähte auch längs gegeneinander etwas verschieben können.

Diese Sechseckbündel können daher, ähnlich wie Seile, über Rollengänge und Hilfsstege als Kabel für Hängebrücken verlegt werden. Da heute sehr große Drahtlängen geliefert werden, brauchen die Drähte innerhalb des Kabels nicht gestoßen werden.

Aus diesen Sechsecken kann man nun mit Futterleisten am Rand ein tadelloses rundes Kabel zusammenbauen (Fig. 7), bei dem sich beim späteren Zusammenpressen und Umwickeln keine Drähte mehr gegenseitig verschieben müssen. Für große Kabel können außen sogar Teile von Sechsecken als Bündel zugelegt werden (Fig. 8), wenn man entlang der Teilungslinie des Sechseckes

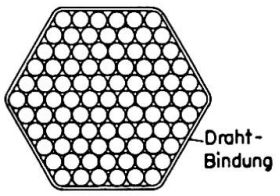

Fig. 6. Sechseckiges Drahtbündel, straff umwickelt, läßt sich wie ein Seil verlegen.

Fig. 7. Kabel aus sechseckigen Drahtbündeln.

a = Sechseckige Drahtbündel.
b u. c = Futterstäbe, z. B. aus Beton.

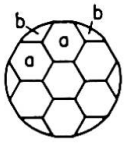

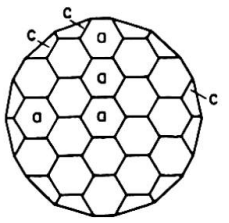

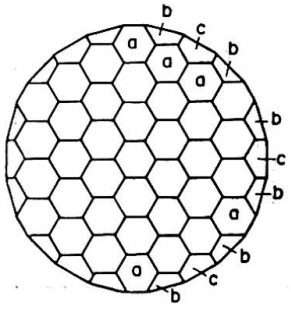

Fig. 8. Kabel aus 37 vollen, sechseckigen Bündeln a, am Rand ergänzt mit Teilbündeln.

a = Sechseckige Drahtbündel, 37 Stück.
b = ⅓-Bündel, 12 Stück.
c = ½-Bündel, 6 Stück.

in gewissen Abständen biegesteife Platten legt, welche die Form des Teilbündels sichern. Diese biegesteifen Platten werden nach der Montage des Kabels kurz vor dem endgültigen Umwickeln wieder weggenommen.

Parallele Drähte haben den großen Vorzug, daß der Elastizitätsmodul innerhalb der Gebrauchsspannungen konstant und hoch ist, während bei Seilen die Spannungsdehnungslinie am Anfang etwas flach verläuft (Seilreck), dann nur kurz gerade ist und frühzeitig in den gekrümmten Bereich der plastischen Verformungen übergeht. Der E-Modul ist dabei im Mittel wesentlich niedriger als beim geraden Draht. Die Verformungen von parallelen Drahtkabeln sind daher kleiner und lassen sich zuverlässiger berechnen als diejenigen von Seilen.

Derartige Hängebrückenkabel haben folgende Vorteile:

1. Hoher konstanter E-Modul, also klar berechenbare, kleine Verformungen.
2. Hohe Ermüdungsfestigkeit, auch an den Verankerungen, daher volle Ausnutzbarkeit der Drahtfestigkeit, selbst bei Brücken mit leichten Fahrbahnen.
3. Einwandfreier und haltbarer Korrosionsschutz in allen Teilen.
4. Einfache Herstellung und verhältnismäßig niedrige Kosten.

Schrifttum

1. H. K. Havemann: «Die Seilverspannung der Autobahnbrücke über die Norderelbe. — Bericht über Versuche zur Dauerfestigkeit der Drahtseile.» Der Stahlbau, 31 (1962), Heft 8, S. 225—232.
2. F. Leonhardt und W. Andrä: «Fußgängersteg über die Schillerstraße in Stuttgart.» Die Bautechnik, 39 (1962), Heft 4, S. 110—116.
3. K. Schaechterle und F. Leonhardt: «Hängebrücken III.» Die Bautechnik, 19 (1941), Heft 12/13, S. 125—133.

Zusammenfassung

Die bisher üblichen Seile zeigen an ihrer Verankerung mit Seilköpfen eine verhältnismäßig niedrige Ermüdungsfestigkeit, so daß die Kabel großer Brücken oft im Hinblick auf die erwartete Schwingbreite der Spannungen nicht voll ausgenützt werden. Es wird gezeigt, wie Kabel auf kleinstem Raum verankert werden können und wie dabei durch geschickte Formgebung der Anker die Schwingbreite um etwa 40% gesteigert werden kann. Ferner wird ein günstiges Herstellungsverfahren für große Paralleldrahtkabel aus sechseckigen Drahtbündeln beschrieben.

Summary

In large suspension bridges built hitherto with ropes it has not been possible to utilise fully the dynamic stress range permitted in the cable, since the anchor details of the ropes have a lower fatigue strength than the wire in the rope.

The paper shows how the anchor detail may be made smaller and the range of fatigue stress increased by 40 per cent.

In addition the production of large parallel cables composed of small hexagonal strands is described.

Résumé

Dans les grands ponts suspendus, la résistance à la fatigue des câbles au droit de leur culot d'ancrage est relativement faible, ce qui interdit souvent de tirer pleinement parti de leur résistance à cause de la variation des contraintes. Dans ce mémoire, il est montré comment on peut réaliser un ancrage de plus petites dimensions et ainsi augmenter en même temps de 40% l'amplitude des contraintes. On décrit en outre un procédé de fabrication de gros câbles à fils parallèles composés de torons hexagonaux.

IId4

The Behaviour of Steel Beams Under Slow Repeated Loading

Le comportement des poutres métalliques soumises à des répétitions de charge lentes

Das Verhalten von Stahlträgern unter langsam wiederholter Belastung

J. W. RODERICK
Professor
B. RAWLINGS
University of Sydney, Sydney, N.S.W., Australia

Introduction

In the investigation described in this paper the load deformation relationship and the mode of failure have been determined for a series of mild steel flexural members subjected to slow repeated loading of sufficient magnitude to produce some degree of plasticity. Some tests have been carried out on plain bars but the greater number were on specimens with a weld at the centre of the span. The frequency of loading, namely 2000 cycles per day, closely corresponds to that adopted by BAIRSTOW[1]) in his classical series of tests on axially loaded specimens. In the early tests, commenced some years ago, work was confined to central concentrated loads applied to plain and welded specimens which had been cut out of the flanges of an 8 inch × 6 inch rolled steel joist. These early tests provided some guidance for a more recent programme, in which both plain and welded specimens are being loaded under central and two-point loads. As the mode of testing is slow, attention so far has been confined to tests under severe conditions in which the beams are loaded well beyond the yield moment. Ultimately it is intended to test additional specimens at lower loads to determine the effect of reducing the degree of overstrain.

Description of Tests

a) Testing Machine

The testing machine used for loading the specimens is shown in Fig. 1. The specimen, of rectangular cross section and 20 inch (50.8 cm) simply supported span, rests on knife edges on rollers and is loaded to bend about the major axis, by dead load, applied and removed by an overhead rocking beam. The motion of this rocking beam is actuated by an eccentric which is

---

[1]) L. BAIRSTOW: "The Elastic Limits of Iron and Steel under Cyclical Variations of Stress." Phil. Trans. Roy. Soc., A. Vol. 210, 1909—1910, p. 35.

chain-driven from a 1000 to 1 reduction gearbox driven by a 1425 r.p.m. squirrel cage induction motor. The frame supporting the gearbox, motor and rocking beam is made independent of that supporting the specimen in order to isolate the specimen from any vibration which might develop.

An overload cutout is installed, to stop the motor in the event of any seizure of the equipment, and limit switches set below the specimen will stop the machine if the specimen deforms to an extent in excess of a selected maximum value. Locating stops are also provided to prevent the specimen from wandering whilst the test is in progress.

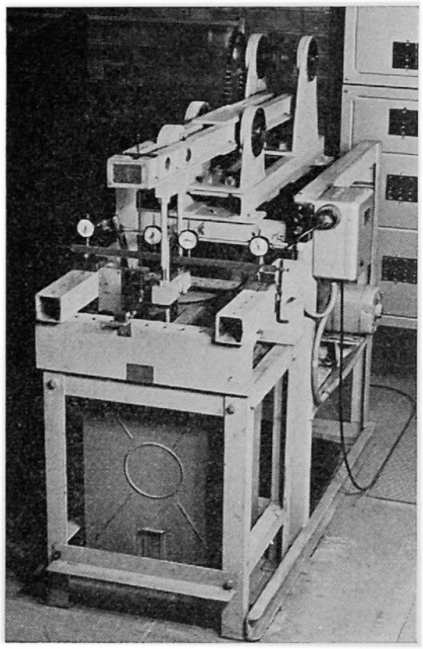

Fig. 1.

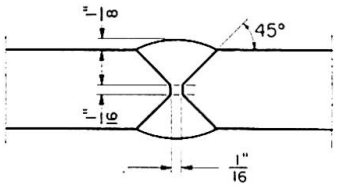

Fig. 2.

Deflections of the beams were recorded by four 0.001 inch dial gauges, mounted above the specimen supports and at points 2 inches from each side of the centre of the span. For the purposes of plotting graphs, the beam deflection was taken as the mean of the inner gauge readings minus the mean of the readings of the support gauges. A cycle counter of the manual reset type was fitted to operate from the rocker beam.

The cycle selected for these tests was such that the load was applied to the specimen for approximately 50% of the total time.

b) Specimens

In an early series of tests, the specimens were cut from the flanges of a length of 8 inch × 6 inch @ 35 lb./ft. British Standard rolled steel joist. The flanges were removed and one was oxy-cut into parallel strips, subsequently ground to provide specimens $^3/_4$ inch × $^1/_2$ inch (1.90 cm × 1.27 cm) in cross section. The second flange was divided transversely at the centre, double V butt-welded, and cut into specimens ground to the same section. These latter

specimens proved to have been badly welded, and were used mainly for a pilot run on the machine. In addition a number of plain specimens were tested, some as static control specimens, some under repeated loading, and using a central concentrated load in both cases.

As it was felt desirable to study behaviour under conditions of pure flexure, two-point load spreaders were introduced and a second and more extensive series of tests was planned. In this case, specimens were cut from a piece of $^7/_8$ inch thick mild steel plate and both plain and welded specimens were prepared. For the latter, a 2′ 9″ length was taken, cut down the centre and prepared for welding. A double V-butt arc weld was made in accordance with Fig. 2, the first run being with a number 10 "Arcraft" E.M.F. electrode and subsequent runs with a number 8 electrode. These electrodes were claimed by the manufacturers to have the following properties:

Yield stress	=	25—27 ton/in.^{2}
Ultimate stress	=	32—36 ton/in.^{2}
Izod impact	=	45 ft.-lb.

Finally the plate was divided by flame cutting into thirty specimens. These were ground down to the dimensions of $^3/_4$ inch depth $\times$ $^1/_2$ inch width, the $^3/_4$ inch being in the direction of the thickness of the plate. The reduction of section in the last few passes of the specimens through the grinder was kept to a minimum in order to reduce the risk of severe work-hardening of the surface. It should be emphasised that the welding operation was carried out manually and no special care was taken to ensure freedom from defects. An X-ray of the weld revealed that the penetration had been complete but there was some evidence of a few small inclusions, and the presence of these was confirmed after the beams were tested and broken apart.

The welded specimens were subsequently tested with the weld at the centre of the span, under central or two-point loading. In the hope of improving the performance under repeated loading, a number of the welded specimens were normalised at 900° C for an hour prior to the final grinding process, and these also were ground carefully to the same surface finish as the other specimens. These specimens were subsequently tested under repeated central concentrated load.

Behaviour of Specimens

a) Static Tests

The details of the various specimens and results of static tests are summarised in Table 1. Typical curves plotted from these results are shown in Fig. 3. The value of full plastic moment accepted for the central point load tests was that corresponding to the point P (Fig. 3) at which the curve just entered the inclined region of strain-hardening behaviour. It will be seen that this value

Table 1. Static Test Results

Specimen Number	Type	Breadth b inches	Overall Depth $2d$ inches	Plastic Section Modulus $S=bd^2$ inches^3	Loading Condition	Load Corresponding to Full Plasticity lb.	Full Plastic Moment of Resistance M_p kip-in.	$\frac{M_p}{S}$ kip/sq. in.
FA 5	Plain	0.492	0.745	0.0681	Single point	500	2.50	36.8
P 2	Plain	0.502	0.751	0.0710	Two point	690	2.76	38.8
P 3	Plain	0.501	0.751	0.0708	Single point	540	2.70	38.2
W 1	Welded	0.502	0.752	0.0711	Single point	620	3.10	43.5
W 2	Welded	0.501	0.751	0.0708	Two point	715	2.86	40.5
W 19	Welded-normalised	0.467	0.726	0.0615	Single point	440	2.20	35.8

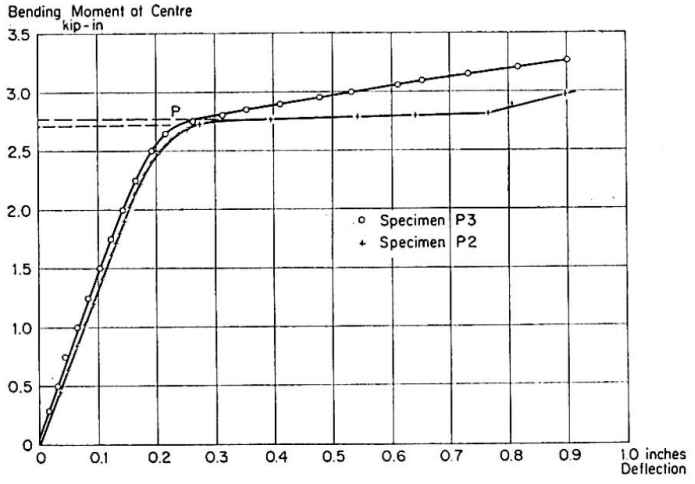

Fig. 3.

agreed fairly closely with that obtained from a uniform flexure test on the same type of specimen.

b) Tests under Repeated Loading

The results of the repeated loading tests, including details of the specimen dimensions, applied load and number of cycles to failure, are summarised in Table 2.

It will be observed that in all cases the loads applied to the specimen produced maximum moments exceeding that which on the basis of the simple plastic theory, would be expected to cause extreme fibre yielding, having in mind that no pronounced upper yield effects were observed in the static tests. Consequently in the loading of the specimens prior to repeated loading some creep occurred and continued until the first removal of the applied load. When the repeated loading was commenced, deformation increased rapidly in the first few cycles, but the rate of increase diminished considerably after about twenty applications of the load, and for the principal part of the test the incremental deflection with each cycle was extremely small.

After many cycles of load the final stage of each test was reached when a crack began to develop in the material. The first detectable sign of failure, both in the single and two point loading specimens, was the appearance of a fine transverse crack in the extreme tensile fibres near the centre of the span. This crack gradually penetrated into the material, until it progressed through approximately half of the depth of the section. This phase was accompanied by an initially slight, and ultimately rapid, increase in deflection under load, until the stage was reached when the machine was stopped by the tripping of the limiting switch. The machine was then readjusted and the loading continued until the specimen could no longer support the load and simply deformed in order to allow the loading bucket to follow the motion of the crosshead and overhead beam. The number of cycles was then recorded, and the test stopped; this stage was regarded as failure of the specimen.

The final phase of crack propagation developed over many cycles of loading, and in some cases, over a period of some months. At no time did any specimen develop brittle characteristics and snap catastrophically and in many cases the specimens carried the full load even when the crack had penetrated through more than half the depth of the specimen. Even when the tests were abandoned, some slight elastic recovery of each specimen was observed when the bucket and beam were raised.

It is convenient to represent the readings of progressive deflection against the number of cycles, as shown in Fig. 4, using a logarithmic scale as abscissa, and linear scale for ordinates. The graphs as shown are at arbitrary heights but the true initial values of deflection at the commencement of testing are given in Table 2.

Table 2. Repeated Loading Test Results

Specimen Number	Type	Breadth b inches	Overall Depth $2d$ inches	Plastic Section Modulus $S = bd^2$ inches^3	Loading Condition	Full Plastic Moment M_p kip-in.	Applied Repeated Load lb.	Corresponding Maximum Moment M kip-in.	$\frac{M}{M_p}$	$\frac{M}{S}$ kip/sq. in.	Number of Cycles to Failure	Initial Value of Deflection inches
FA 1	Plain	0.492	0.745	0.0681	Single point	2.50	460	2.30	0.92	33.7	3,689,392+	0.1504
FA 5	Plain	0.492	0.745	0.0681	Single point	2.50	520	2.60	1.04	38.1	382,265	0.2997
P 5	Plain	0.500	0.750	0.0703	Two point	2.74	700	2.80	1.02	39.8	109,884	0.6080
W 16	Welded	0.500	0.750	0.0703	Single point	3.06	624	3.12	1.02	44.5	29,245	0.3788
W 25	Welded	0.505	0.750	0.0711	Single point	3.10	593	2.96	0.96	41.7	56,842	0.2564
W 3	Welded	0.502	0.751	0.0709	Single point	3.09	572	2.86	0.93	40.5	50,557	0.1974
W 12	Welded	0.501	0.751	0.0708	Single point	3.08	530	2.65	0.86	37.5	161,632	0.2137
W 6	Welded	0.501	0.751	0.0708	Two point	2.86	700	2.80	0.98	39.6	21,852	0.5172
W 5	Welded	0.501	0.751	0.0708	Two point	2.86	665	2.66	0.93	37.7	71,014	0.2816
W 15	Welded	0.501	0.750	0.0705	Two point	2.85	630	2.52	0.89	35.7	63,332	0.2225
W 26	Welded	0.500	0.750	0.0703	Two point	2.84	595	2.38	0.84	34.0	108,331	0.1801
W 19	Welded, normalised	0.467	0.727	0.0616	Single point	2.20	440	2.20	1.00	35.8	16,561	0.2024
W 20	Welded, normalised	0.467	0.727	0.0616	Single point	2.20	418	2.09	0.95	33.9	18,455	0.1549
W 22	Welded, normalised	0.467	0.727	0.0616	Single point	2.20	396	1.98	0.90	32.2	31,661	0.1481

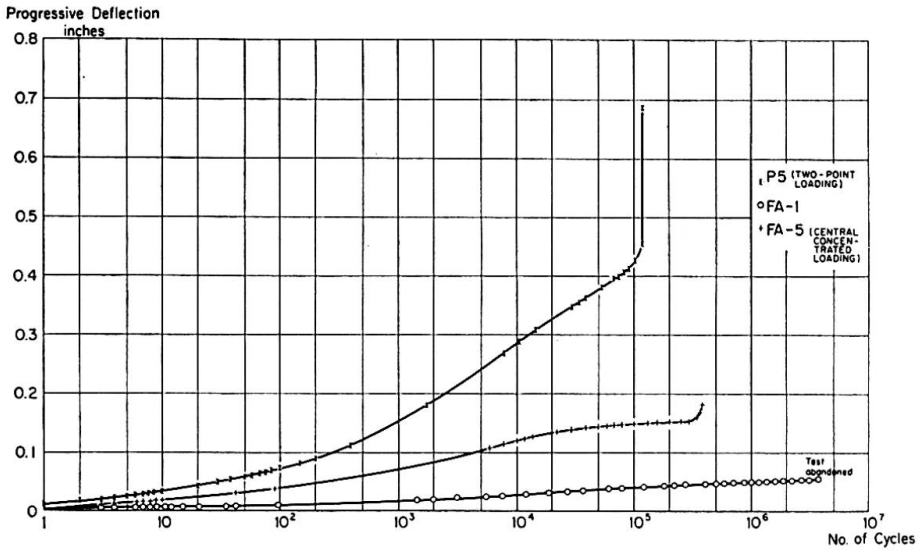

Fig. 4a.

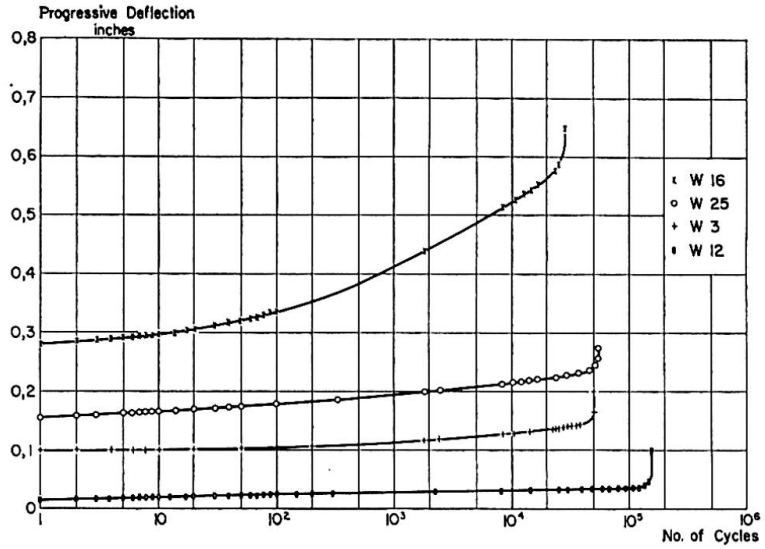

Fig. 4b.

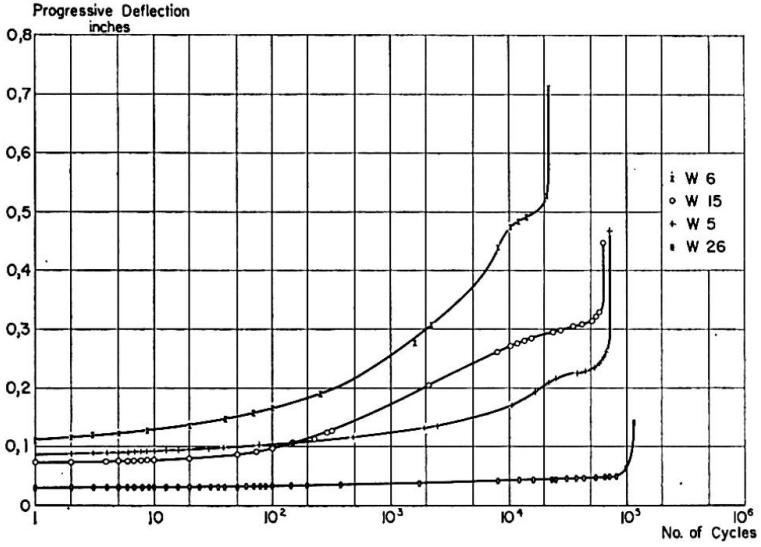

Fig. 4c.

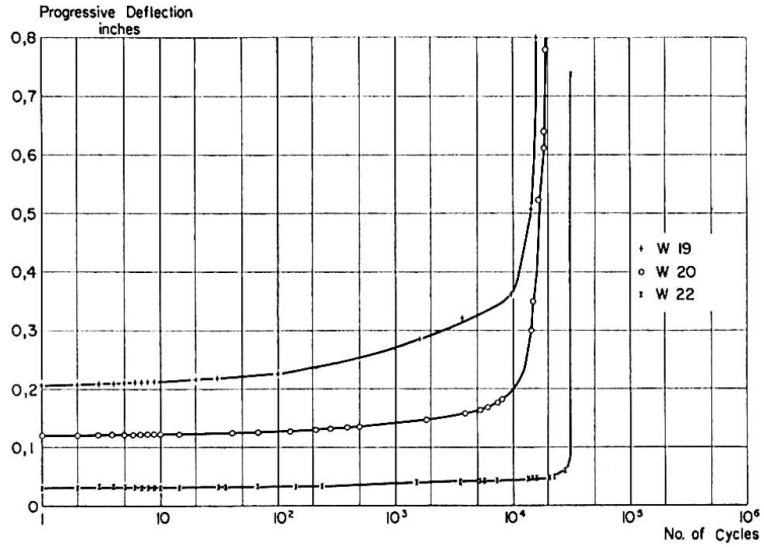

Fig. 4d.

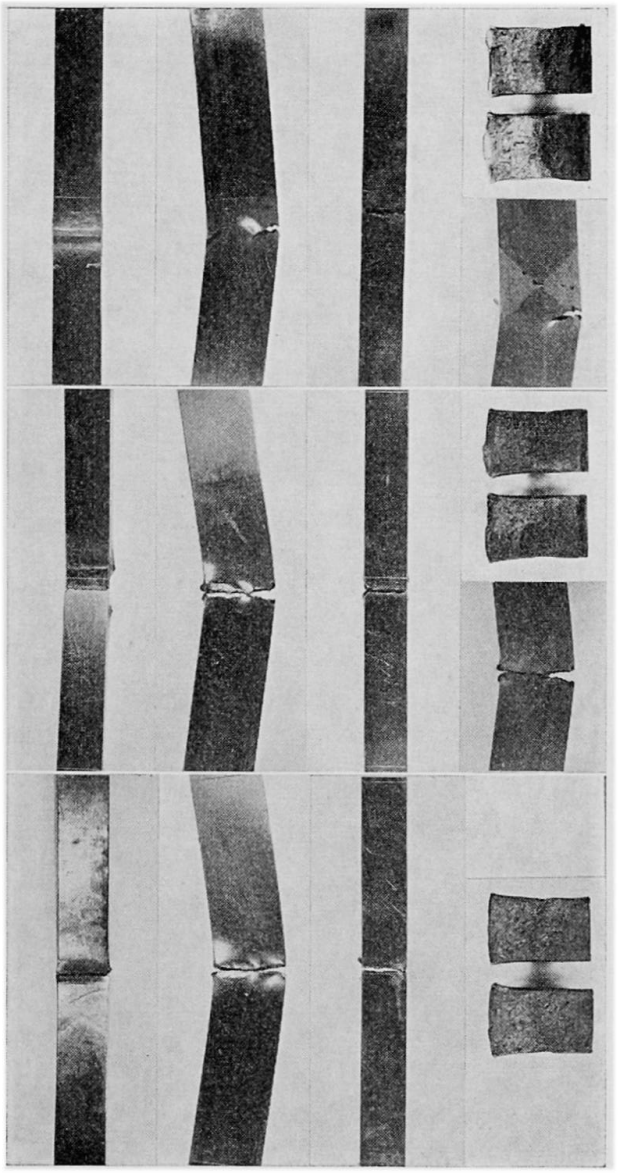

Specimen FA-5 Specimen W 20 Specimen W 15

Fig. 5a. Fig. 5b. Fig. 5c.

In a number of the tests, readings were taken of the beam deflections both when the load was applied and when it was subsequently removed. These can be plotted as two curves, the vertical intercept between which was found to be constant throughout each test, suggesting that at all stages the recovery was elastic. For a beam of linear and elastic material, the magnitude δ would be given by the expression

$$\delta = \frac{472\,P}{3\,E\,I}$$

in inch units, for the central load tests, and by

$$\delta = \frac{448\,P}{3\,E\,I}$$

for the two point loading tests, where P, E and I are respectively the applied load, elastic modulus and second moment of area of the testpiece. The values of E, as derived from these expressions and using the test results, ranged between 27.3×10^6 p.s.i. and 30.8×10^6 p.s.i., so that in each case the magnitude of the recovery can be said to agree satisfactorily with that expected on the basis of linear elastic behaviour.

Nature of Fractures

A number of photographs of specimens after testing showing elevations, top and underneath views and fracture surfaces are shown in Fig. 5. It will be evident that in all cases the region of the specimen adjacent to the fracture underwent considerable plastic deformation, and this was accompanied by lateral flow of the material, resulting in the large distortions of the cross-sections. The distorted surfaces are also clearly seen in the elevations. In a number of specimens rippling of the compression face was evident, and in others, some fine transverse cracks could be observed in the compression face when the specimen was closely examined. It will be observed from the photograph of specimen W 20 (Fig. 5b) that, even when the specimen was broken apart prior to photographing, there was some ductility of the remaining material as the two parts do not mate together precisely at the top.

Under single point loading conditions, the cracks were located at a section near the centre, but in most cases displaced approximately $^1/_2$ inch away and near the extremity of the welded zone. In the case of the welded specimens subjected to two point loading, the cracks again frequently developed to one side of the centre line of the span, as is shown in Fig. 5c. (Specimen W 15.) The unwelded specimen subjected to two point loading developed a crack which originated under one of the loading points, in the tensile fibre. The crack propagated from one of the scribed lines used for marking out the

specimen prior to testing. Cracks in the specimens propagated vertically, and often appeared to emanate from a small weld defect such as an inclusion near the tensile face. It will be seen from the photographs in Fig. 5 which show elevations of typical welded specimens after etching with 10 per cent nitric acid in methylated spirit, that the cracks all originated within the welded zone, although in many cases they subsequently penetrated regions of unwelded material.

If attention is directed to the sectional views, which were taken after the specimens were broken apart in a vice, it will be observed that in some striations occurred consistent with the progressive nature of the cracking. These are particularly noticeable in the case of specimen FA-5. The fractures were crystalline in appearance, the lighter colour occurring in the region which was freshly broken.

Life of Specimen as a Function of Loading

The test results are summarised in Fig. 6. Here, the number of cycles to failure are plotted on a logarithmic axis, against the applied maximum moment divided by the plastic section modulus of each specimen. These same results are plotted again in Fig. 7, the ordinate being the maximum applied moment divided by the full plastic moment of a specimen of the same dimensions, as determined from the static tests. In both figures the relationship between the logarithm of the life of a specimen, and loading, will be seen to be sensibly linear.

It will be observed that the curves for two point and central point loading specimens agree fairly closely, when allowance is made for the different values of full plastic moment of resistance. If it is assumed that the section where

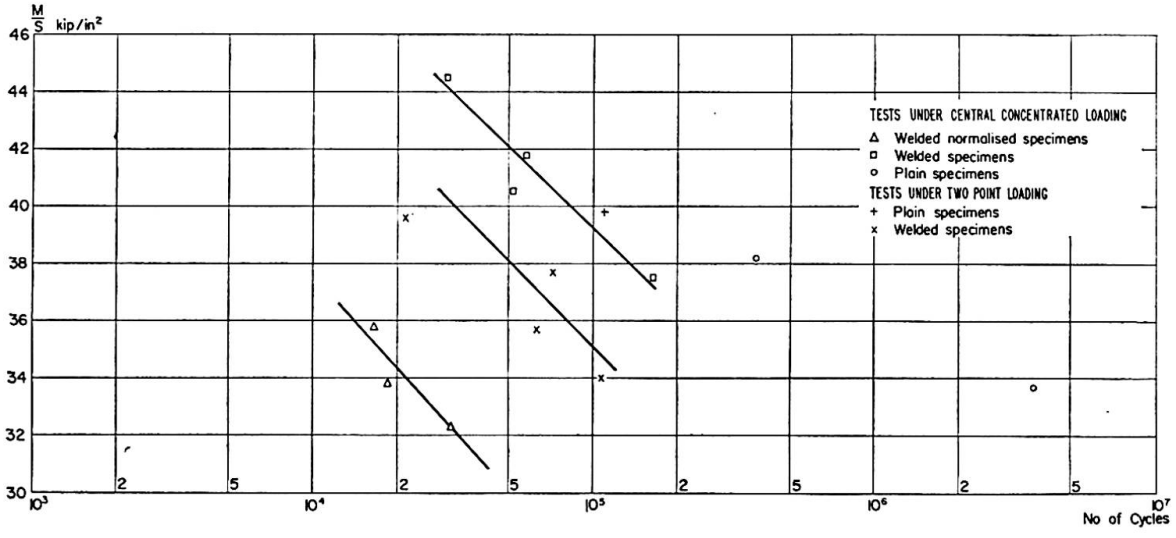

Fig. 6.

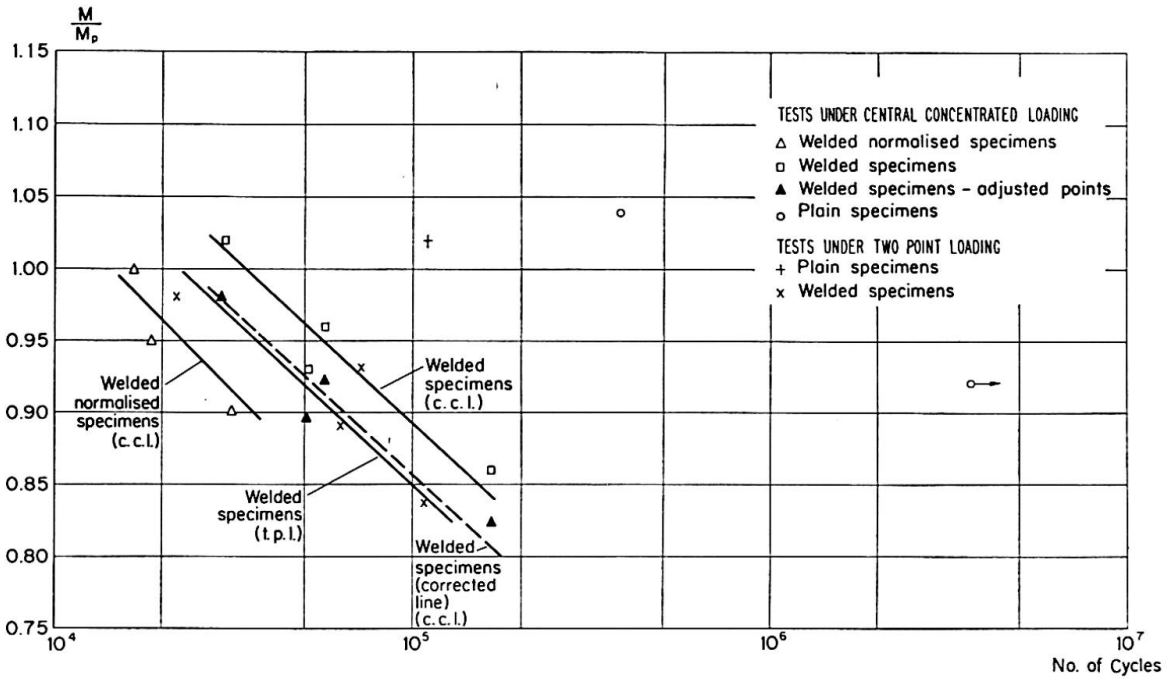

Fig. 7.

cracking occurs is at the extremity of the weld as is suggested by the photographs of the etched specimens, it will be seen that at these sections, the moment is only 96 per cent of the central moment, consequently the curve in Fig. 7, for the welded central load tests will be displaced downwards to the position shown by the broken line. The results of the central load and two-point load tests then agree very closely.

It is also interesting to note that, while the process of normalising the welded specimens lowered the yield point of the material their life appeared to be slightly reduced.

Conclusions

Although at this stage, any conclusions must be regarded as a little tentative, the tests to date have given a great deal of qualitative information on the behaviour of steel members under many cycles of slow repeated loading, and it is hoped that further work will enable the relationship between the applied moment and life of the specimen to be determined over a wide range of moments.

It can be said, however, that the material does not behave in a brittle manner with little plastic deformation during the course of repeated loading, and catastrophic collapse does not take place. Even when testing was discontinued and the specimens were withdrawn from the machine and broken in a vice, they exhibited some residual ductility. In addition, though there were some imperfections in the welding of the specimens tested, these did not lead to collapse of the specimens at a very early stage.

As has been mentioned, it is planned in future testing, to extend the range of applied moments to include both high values well into the strain-hardening range, and lower values closer to the yield moment, and to conduct tests on specimens having close control on the material and welding, under intermittently applied, and reversing moment, and under programmed loading.

Acknowledgements

The Authors acknowledge the assistance of Messrs. J. J. Reilly and R. Kwan, students in the Department of Civil Engineering, University of Sydney, who conducted a number of the tests as part of an undergraduate thesis exercise.

Summary

An account is given of a series of preliminary tests on rectangular, simply supported mild steel beams subjected to many cycles of intermittent transverse loading, applied at $1^1/_2$ cycles per minute. The results suggest that the life of a specimen as plotted on a logarithmic scale, bears a linear relationship to the applied moment. The behaviour of both plain and welded specimens is described, both prior to, and after the development of cracking.

Résumé

Les auteurs présentent une série d'essais préliminaires exécutés sur des éprouvettes fléchies en acier doux, de section rectangulaire et simplement appuyées, soumises à un grand nombre de cycles de chargements transversaux discontinus appliqués à raison de 1½ cycle par minute. Il ressort des résultats que le nombre de cycles supporté par l'éprouvette, si on le rapporte à une échelle logarithmique, peut s'exprimer linéairement en fonction du moment appliqué. On décrit le comportement d'éprouvettes ordinaires et d'éprouvettes soudées avant et après le début de la fissuration.

Zusammenfassung

In einer Reihe von Vorversuchen wurden einfach gelagerte Prüfstücke aus St 37 mit rechteckigem Querschnitt einer großen Zahl von intermittierenden Lastwechseln auf Biegung mit 1½ Perioden pro Minute unterworfen. Die Versuche ergaben einen linearen Zusammenhang zwischen den auf einer logarithmischen Skala aufgetragenen Lastwechseln, die vom Prüfstück ausgehalten wurden, und dem belastenden Moment.

Der Bericht umfaßt das Verhalten von gewöhnlichen und von in Feldmitte geschweißten Prüfstücken, vor und nach dem Anriß.